

Latest three-flavor neutrino oscillation results from NOvA

Liudmila Kolupaeva, for the NOvA collaboration*

The Joint Institute for Nuclear Research

E-mail: ldkolupaeva@yandex.ru

The NOvA experiment is a long-baseline neutrino oscillation experiment that uses the upgraded NuMI beam from Fermilab to detect both electron appearance and muon disappearance. NOvA employs two functionally identical detectors: a Near Detector, located at Fermilab, and a Far Detector, located at Ash River, Minnesota over an 810 km baseline. NOvA's primary physics goals include precision measurements of neutrino oscillation parameters, such as θ_{23} and the atmospheric mass-squared splitting, along with probes of the mass hierarchy and the CP violating phase. This document is devoted to the latest NOvA measurements [1] of the neutrino oscillation parameters using neutrino and antineutrino disappearance and appearance.

*European Physical Society Conference on High Energy Physics - EPS-HEP2019 -
10-17 July, 2019
Ghent, Belgium*

*Speaker.

1. Introduction

NOvA [2] is a long-baseline accelerator neutrino experiment devoted to studying the properties of neutrino oscillations. It consists of two functionally identical tracking calorimeter detectors. The NuMI facility [3] at FNAL (USA) creates a muon (anti-)neutrino beam which travels 810 km through the Earth's crust to the Far Detector, which is placed at Ash River (Minnesota, USA).

The proton NuMI beam with 120 GeV energy is delivered to the carbon target. This interaction produces mesons which decay into leptons and neutrinos. The resulting beam composition is as follows: 95% ν_μ , 4% $\bar{\nu}_\mu$, 1% ν_e (93% $\bar{\nu}_\mu$, 6% ν_μ , 1% ν_e in the case of antineutrino beam). The sign of the neutrino beam (whether it consists of neutrinos or antineutrinos) depends on the polarity of the magnetic horns which are used for focusing mesons with a specific charge.

NOvA's design power is 700 kW, which means 6×10^{20} protons delivered to the target (POT) per year. Currently NOvA has collected 8.85×10^{20} POT with neutrino beam and 12.33×10^{20} POT with antineutrino beam.

The experiment uses two detectors which are placed 14.6 mrad off the beam axis. This scheme helps to obtain narrow energy peak close to 2 GeV. The Near Detector (ND) has dimension $4.2 \text{ m} \times 4.2 \text{ m} \times 16 \text{ m}$ and 300 t mass. It is placed about 1 km after the target and used for measuring the neutrino flux before oscillations. The Far Detector (FD) is used for measuring the neutrino flux after oscillations at a distance 810 km. It has dimensions of $15.6 \text{ m} \times 15.6 \text{ m} \times 60 \text{ m}$ and a 14 kt mass.

Both detectors consist of PVC cells filled with a liquid mineral oil based scintillator. Each cell contains a wavelength-shifting fiber loop which is connected with 32-pixel avalanche photodiodes used for readout electronics. Due to the small size of the cells ($4.2 \text{ cm} \times 6 \text{ cm}$) the detector segmentation is very good. Cells are collected into planes. Planes with different orientations alternate each other.

The NOvA detectors were designed to observe electron and muon (anti-)neutrinos. In order to identify and classify events the Convolutional Visual Network [4] is used. It is an image recognition technique which uses the map of event hits as an input.

Resulting neutrino energy spectra at the FD are sensitive to certain oscillation parameters: Δm_{32}^2 , θ_{23} , δ_{CP} and the neutrino mass hierarchy. This document will describe NOvA's result [1] produced with data collected between July 2013 and February 2019 with neutrino and antineutrino beam.

2. Far Detector and Near Detector data

Similar detector construction allows for the application of the so-called extrapolation procedure: a data-driven technique for producing predictions in the FD. The high statistics of the ND data are used for constraining the Monte-Carlo. Corrected Monte-Carlo is extrapolated to the FD and is used for the data fit. It helps to reduce the size of cross-section and flux systematic uncertainties. A full list of systematic uncertainties for the measured parameters is shown in Figure 1.

NOvA's three-flavor oscillation analysis consists of two main interaction channels: electron neutrino appearance and muon neutrino disappearance.

Source of Uncertainty	$\sin^2\theta_{23}$ ($\times 10^{-3}$)	δ_{CP}/π	Δm_{32}^2 ($\times 10^{-3}$ eV ²)
Beam Flux	+0.42 / -0.48	+0.0088 / -0.0048	+0.0016 / -0.0015
Detector Calibration	+6.9 / -6.1	+0.15 / -0.023	+0.024 / -0.029
Detector Response	+1.9 / -0.99	+0.055 / -0.054	+0.0027 / -0.0034
Muon Energy Scale	+2.6 / -2.1	+0.015 / -0.0026	+0.01 / -0.012
Near-Far Differences	+0.56 / -1.1	+0.11 / -0.064	+0.0033 / -0.0013
Neutrino Cross Sections	+4.2 / -3.5	+0.085 / -0.072	+0.015 / -0.014
Neutron Uncertainty	+6.4 / -7.9	+0.002 / -0.0052	+0.0028 / -0.01
Normalization	+1.4 / -1.5	+0.031 / -0.024	+0.0029 / -0.0027
Systematic Uncertainty	+9.6 / -11	+0.21 / -0.11	+0.032 / -0.035
Statistical Uncertainty	+22 / -29	+0.9 / -0.27	+0.064 / -0.059

Figure 1: Systematic uncertainties for the joint $\nu_e + \nu_\mu$ analysis with neutrino and antineutrino beam.

In the case of muon neutrino disappearance result, we split the ND reconstructed energy spectrum into 4 quartiles. This decision is based on the reconstructed hadron energy fraction to the full reconstructed neutrino energy. Quartile no.1 has the best energy resolution ($\sim 6\%$) and the lowest hadron energy fraction. On the contrary, quartile no. 4 has the worst energy resolution ($\sim 12\%$) and the highest hadron energy fraction. The resulting measured spectra of ND ν_μ Charged Current (CC) candidates are shown in the Figures 2 - 3.

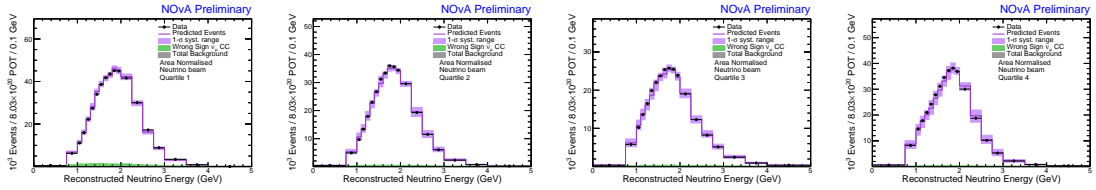


Figure 2: Measured reconstructed energy spectra of ND ν_μ CC events (dots) compared to the ND Monte-Carlo (violet line).

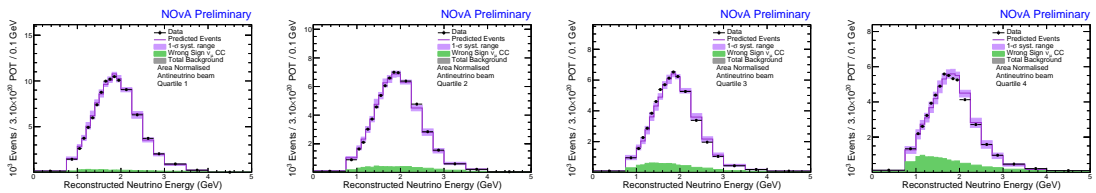


Figure 3: Measured reconstructed energy spectra of ND $\bar{\nu}_\mu$ CC events (dots) compared to the ND Monte-Carlo (violet line).

Each quartile is separately extrapolated to the far detector. ND ν_μ ($\bar{\nu}_\mu$) events are the source of ν_μ ($\bar{\nu}_\mu$) and ν_e ($\bar{\nu}_e$) signal in the FD. Similarly the ND ν_e ($\bar{\nu}_e$) CC events are the source of background in the FD. Measured spectra of these events are shown in Figure 4. We split these data into two spectra (High and Low PID) based on the CVN score.

In the FD NOvA observed 113 ν_μ CC (102 $\bar{\nu}_\mu$ CC) candidates with a background expectation $4.2^{+0.8}_{-0.6}$ events with neutrino beam and $2.2^{+0.4}_{-0.4}$ events with antineutrino beam. Final ν_μ and $\bar{\nu}_\mu$ spectra are shown in the Figure 5. There are 58 ν_e CC (27 $\bar{\nu}_e$ CC) candidate events with an expected

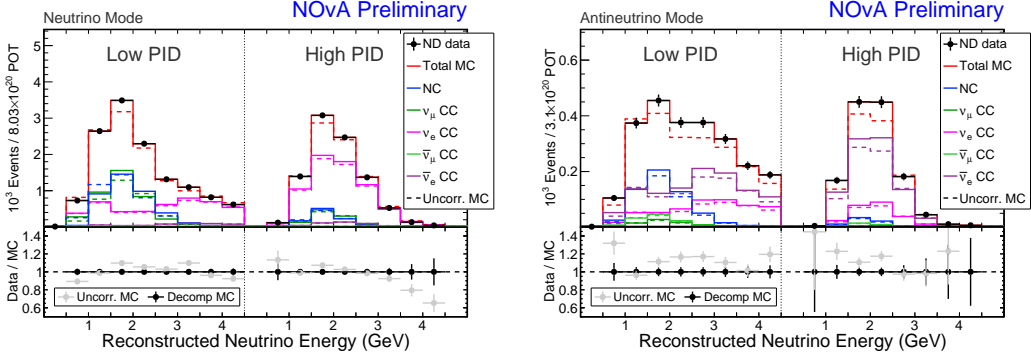


Figure 4: Measured reconstructed energy spectra of ND ν_e CC (left) and $\bar{\nu}_e$ CC (right) events (dots) compared to the ND Monte-Carlo (color lines). Data-driven techniques are used to correct Monte-Carlo in order to match the data. Each category of background is extrapolated separately to the FD.

background of $15.0^{+0.8}_{-0.9}$ and $10.3^{+0.6}_{-0.5}$ events for neutrino and antineutrino beam, respectively. Resulting spectra are shown in Figure 6. This observation provides 4.4σ evidence of $\bar{\nu}_e$ appearance in an initially predominantly $\bar{\nu}_\mu$ beam.

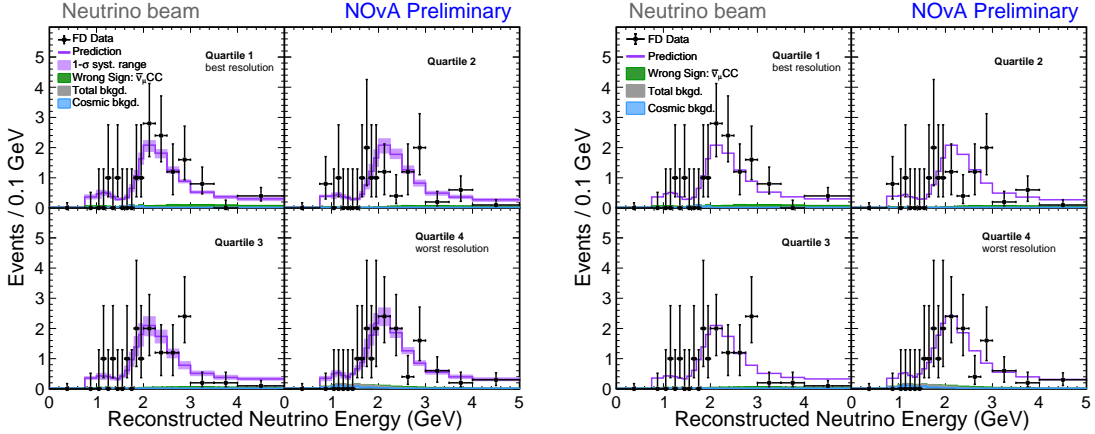


Figure 5: Measured reconstructed energy spectra of FD ν_μ CC (left) and $\bar{\nu}_\mu$ CC (right) events (dots) split into four quartiles.

3. Analysis results

In order to extract the oscillation parameters, a joint fit of spectra in Figures 5 - 6 was performed. Solar oscillation parameters θ_{12} and Δm_{21}^2 were fixed to the PDG values while θ_{23} , Δm_{32}^2 , δ_{CP} and neutrino mass hierarchy were varied. The value of θ_{13} was constrained by reactor experiment measurements. NOvA's analysis is frequentist with profiled systematics and penalty terms.

NOvA's best fit is $\Delta m_{32}^2 = 2.48^{+0.11}_{-0.06} \times 10^{-3} \text{ eV}^2$, $\sin^2 \theta_{23} = 0.56^{+0.04}_{-0.03}$, $\delta_{CP} = 0.0^{+1.3}_{-0.4} \pi$.

It corresponds to the Normal neutrino mass hierarchy and upper octant of θ_{23} ($> \pi/4$). Inverted mass hierarchy is disfavored at 1.9σ . Upper octant of θ_{23} is preferred at 1.6σ , but result is still consistent with maximal mixing at 1.2σ (Figure 8).

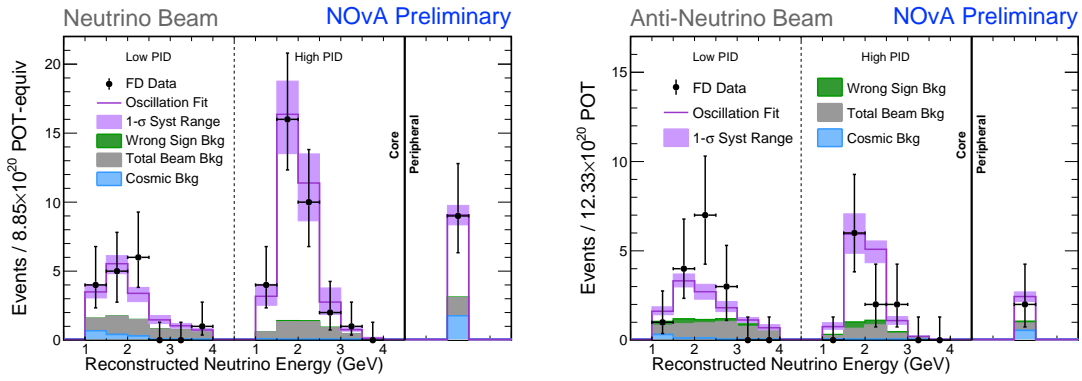


Figure 6: Measured reconstructed energy spectra of FD ν_e CC (left) and $\bar{\nu}_e$ CC (right) events (dots) split into two CVN PID bins and one additional Peripheral bin which collected all uncontained events included in the analysis.

The $1,2,3\sigma$ contours in $\sin^2\theta_{23} - \Delta m_{32}^2$ and $\sin^2\theta_{23} - \delta_{CP}$ are shown in the Figure 7. The large region in Inverted hierarchy at $\delta_{CP} = \pi/2$ was ruled out at $> 4\sigma$.

The exclusion significances at which each value of δ_{CP} , Δm_{32}^2 and $\sin^2\theta_{32}$ is disfavored are shown in the Figure 8. All values of δ_{CP} in the Normal hierarchy and Upper octant of θ_{23} are allowed at 1.1σ .

References

- [1] M. A. Acero *et al.* [NOvA Collaboration], “First Measurement of Neutrino Oscillation Parameters using Neutrinos and Antineutrinos by NOvA,” *Phys. Rev. Lett.* **123**, no. 15, 151803 (2019) doi:10.1103/PhysRevLett.123.151803 [arXiv:1906.04907 [hep-ex]].
- [2] D. S. Ayres *et al.* [NOvA Collaboration], “NOvA: Proposal to Build a 30 Kiloton Off-Axis Detector to Study $\nu_\mu \rightarrow \nu_e$ Oscillations in the NuMI Beamline,” hep-ex/0503053.
- [3] P. Adamson *et al.*, “The NuMI Neutrino Beam,” *Nucl. Instrum. Meth. A* **806**, 279 (2016) doi:10.1016/j.nima.2015.08.063 [arXiv:1507.06690 [physics.acc-ph]].
- [4] A. Aurisano *et al.*, “A Convolutional Neural Network Neutrino Event Classifier,” *JINST* **11**, no. 09, P09001 (2016) doi:10.1088/1748-0221/11/09/P09001 [arXiv:1604.01444 [hep-ex]].

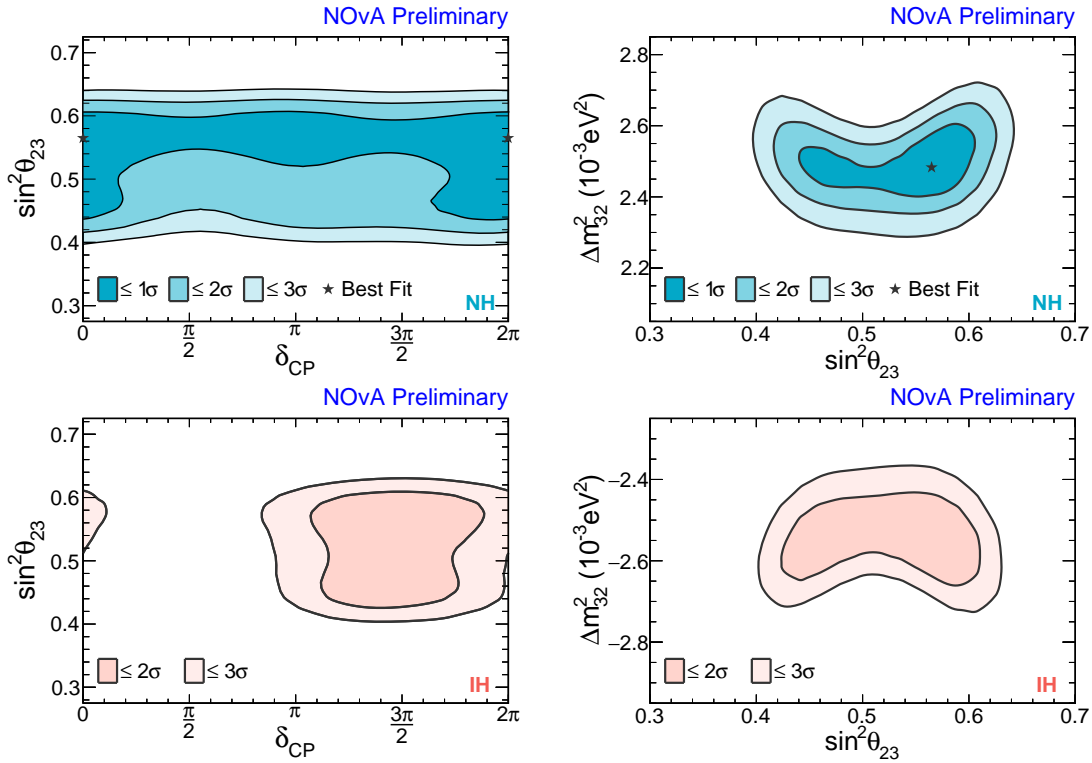


Figure 7: The 1,2,3 σ contours in $\sin^2\theta_{23} - \delta_{CP}$ (left) and $\sin^2\theta_{23} - \Delta m_{32}^2$ (right) in Normal (up row) and Inverted (bottom row) hierarchy. Feldman-Cousins corrections are applied. Best fit is shown by star marker.

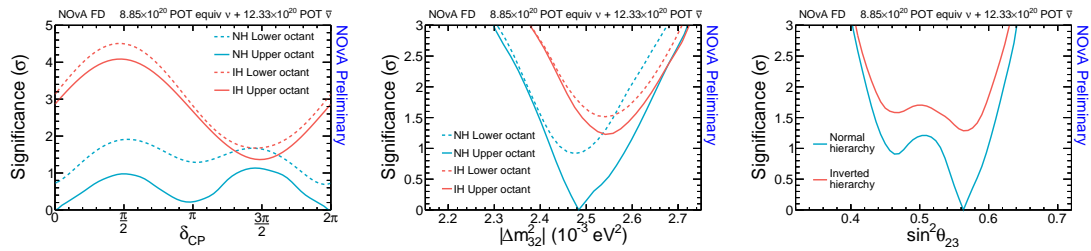


Figure 8: The exclusion significance for each value of δ_{CP} (left), $|\Delta m_{32}^2|$ (middle) and $\sin^2\theta_{23}$ (right) in Normal (blue) and Inverted (orange) mass hierarchy, dashed lines denote the octant (when it's applied).